JOURNAL OF AIRCRAFT
Vol. 38, No. 5, September–October 2001

Correction of Wall Interference in Wind Tunnels: A Numerical Investigation

Giovanni Lombardi* and Maria Vittoria Salvetti†
University of Pisa, 56126 Pisa, Italy
and
Mauro Morelli‡
Council for Scientific and Industrial Research, Pretoria 0001, South Africa

A procedure is described for the correction of wind-tunnel wall interference effects on the experimental measurement of aerodynamic coefficients. The correction is given by the difference between the values obtained in two different numerical simulations: In the first one the flow over the model in free-air conditions is simulated, whereas in the second one, the measured pressure values over the wind tunnel walls are used as boundary conditions. A necessary preliminarly step is the choice of the number, location, and accuracy of the pressure measurements. A strategy is proposed to determine these parameters, based on the same correction procedure in which the experimental part is replaced by numerical simulation. This strategy is applied to the subsonic flow around a complete aircraft configuration by means of a potential flow solver. The sensitivity to the number and location of sensors, as well as to the transducer accuracy, is investigated. Given the desired correction accuracy, the proposed strategy permits identification of suitable configurations with reduced time and computational costs.

Nomenclature

a	=	slot width, m
C_L	=	lift coefficient
C_m	=	pitching moment coefficient
c_p	=	pressure coefficient
E	=	pressure transducer error, kPa
h	=	test section height, m
k	=	parameter depending on the geometry of the slots for the definition of slotted wall boundary conditions
L	=	distance between two slot centers, m
l	=	test section length, m
M	=	Mach number
N_c	=	number of sensors in the cross direction
N_l	=	number of sensors in the longitudinal direction
U_∞	=	freestream velocity, m/s
V_n	=	velocity normal to the wind tunnel walls, m/s
x	=	streamwise coordinate with origin at the model rotation point, m
x_0	=	streamwise coordinate of the inflow tunnel section, m
z	=	vertical coordinate with origin at the model rotation point, m
α	=	angle of attack
ε_{pr}	=	residual error due to wall pressure representation
ε_{tot}	=	global error on aerodynamic coefficients
σ	=	standard deviation of the Gaussian function used to define the longitudinal sensor distribution

I. Introduction

THE interference effect of wind tunnel walls on the flowfield around a model is known to be one of the main sources of error affecting the accuracy of experimental data. The classical correction criteria (see Ref. 1 for a review) are based on theoretical linear models, whose validity is limited to low velocities and angles of attack. However, even in these conditions, the accuracy of these criteria is not high because they do not account for the physical tunnel characteristics. With the introduction of ventilated test sections for high-speed subsonic and transonic testing, new procedures have been devised to extend the classical wall interference methods. Because of the complex nature of the interference, a satisfactory general analytical solution to this problem for ventilated walls is far from being achieved. More recently, new correction methods were introduced,[2] based on more complex procedures, which couple measurements, typically pressure and/or velocity on the wall or in the field, with numerical calculations. The implementation of these procedures is complex because of the uncertainties in the measurements of the wall quantities and because the complexity of the flow calculation. These considerations explain why limiting the model dimensions remains the most used way to avoid unacceptable errors. As an example, in a previous work,[3] an analysis on the wall interference effects in the medium-speed wind tunnel (MSWT) of the CSIR Laboratories, in South Africa, was presented. The MSWT is a closed-circuit variable density transonic wind tunnel, with operational speed from $M = 0.25$ to 1.5; the test section has a 1.5×1.5 m square cross section, and the length is 4.5 m. All four walls are equally longitudinally slotted for a total porosity of 5%. The results showed that very low blockage factors are required to have small wall interference effects. On the other hand, it is evident that it would be attractive to test large models, not only to increase the Reynolds number but, especially, to improve the accuracy of the force measurements and of the model geometry. Thus, it is important to have reliable criteria to choose the model size.

Taking into account this consideration and the increase in computing capabilities, we decided to develop a correction procedure based on pressure measurements on the wind-tunnel walls coupled with a numerical method to evaluate the flow correction.

This procedure is described in detail in Sec. II. In Sec. III, the problem of the definition of the number, location, and accuracy of the pressure measurements on the wind-tunnel walls is investigated. In particular, a sensitivity analysis is carried out in which the experimental pressure measurements are simulated numerically.

II. Correction Procedure

A. Description

The correction methodology employed in the present analysis is a so-called posttest procedure.[1] In these kinds of methods,

Received 31 May 2000; revision received 20 December 2000; accepted for publication 26 December 2000.

*Associate Professor, Department of Aerospace Engineering, Via Diotisalvi 2. Member AIAA.
†Assistant Professor, Department of Aerospace Engineering, Via Diotisalvi 2.
‡Research Engineer, Medium Speed Wind Tunnel, P.O. Box 395.

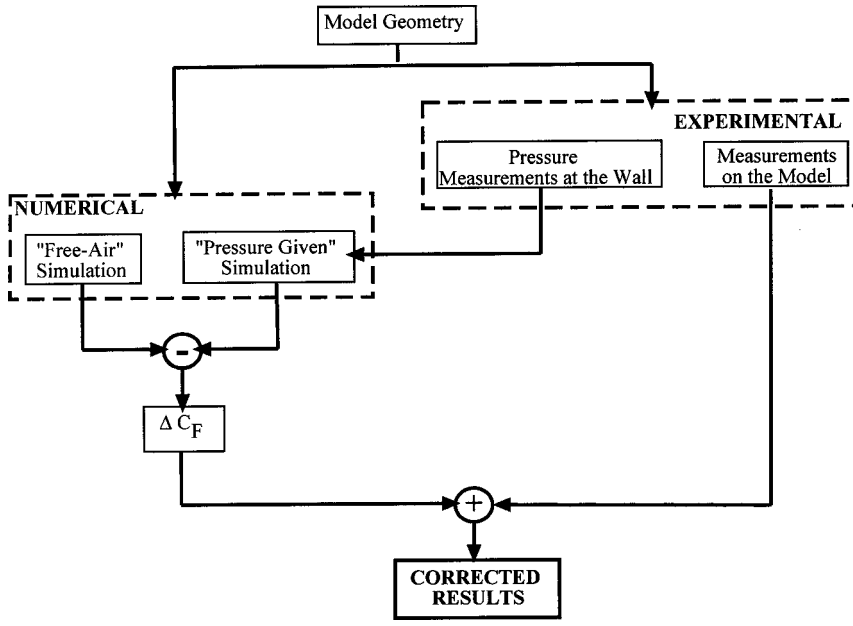

Fig. 1 Scheme of correction procedure.

experimental data must be provided on a control surface located near the wind tunnel walls or directly on them. The experimental data can be pressure, velocity direction, or velocity components. The motivation for the choice of a posttest procedure is that, for slotted walls, accurate analytical boundary conditions are difficult to be devised and used in practice, and this makes pretest corrections not suitable.

In particular, in the present work a one-array correction procedure has been chosen, in which only pressure data are provided at some locations on the wind-tunnel walls.

This approach, although in principle less accurate than two-array corrections, appears to be more affordable from a practical point of view.

Moreover, in two-array procedures, because a larger amount of measurements must be carried out, it is difficult to control the measurement accuracy, and this can significantly decrease the global accuracy of the correction. The scheme of the correction procedure, which is based on the method proposed by Sickles,[4] is shown in Fig. 1.

Once the model geometry is defined, the experimental tests are carried out and, in particular, in addition to the aerodynamic forces acting on the model, the pressure over the wind-tunnel walls is measured at few selected locations. These data are used as boundary conditions in a numerical simulation of the flow around the same geometry [pressure-given simulation (PG)]. Another numerical simulation is carried out in free-air conditions (FA), that is, with a computational domain large enough to avoid spurious boundary effects. The difference between the values of aerodynamic forces obtained in these two simulations is used to correct the experimental data.

B. Numerical and Experimental Issues

Given the described correction scheme, two main aspects must be defined. The first one is the choice of the flow solver adopted in the numerical simulations. The same criteria used in computational aerodynamics are also clearly suitable in this context. Thus, the choice of the numerical solver will depend on the considered configuration and flow conditions (see, for instance, Ref. 5). It is clear that, if one is also interested in correcting drag, a numerical solver of the Navier–Stokes equations should be used, also including a turbulence model. However, the accuracy of the numerical evaluation of drag is far from being assessed even for last generation Navier–Stokes solvers. Thus, in our opinion, the correction of drag still remains an extremely difficult task. Moreover, from a practical point of view, wall interference is only one of the factors that affects drag measurements. Indeed, drag is far more sensitive than lift and pitching moment to other effects (namely, Reynolds number, support interference, wind tunnel turbulence, etc.). For these reasons, we preferred not to address this point in the paper, and this allowed us to use a potential solver for the present analysis. In particular, it is known that potential flow solvers give accurate results for low Mach numbers and angles of attack, with a limited computational cost.

The second issue concerns the experimental measurement of pressure over the wind tunnel walls. In particular, the number and the location of the measurement points must be defined, as well as the required accuracy of the pressure measurements. It seems difficult to find a priori criteria in this case. Indeed, the best choice will depend on many different factors, namely, test section geometry, wind-tunnel wall type, model geometry, and flow conditions. On the other hand, the earlier described correction procedure can be applied only if this aspect is preliminarly defined, and hence a strategy must be devised to obtain a suitable compromise between accuracy and cost of the wall pressure measurements, for each considered test.

In this paper, a strategy is proposed, based on the described correction procedure, in which the experimental part is replaced by a numerical simulation. Thus, an additional computation (denoted as tunnel simulation) is carried out for the flow around the model in the wind tunnel. Then, the pressure values obtained in this simulation are used as boundary condition for the PG numerical simulation. As previously, the difference in the aerodynamic force values obtained in the PG and FA computations will give the desired correction. In this way, an analysis of the sensitivity of the correction to both number and position of the pressure sensors can be carried out. Similarly, the required level of accuracy of the pressure sensors can be estimated. The cost and time needed for this analysis clearly depend on the used flow solver; however, in all cases, they are much lower than those required by a similar study carried out experimentally. Note also that in most cases an experimental sensitivity analysis is unaffordable in practice.

III. Definition of Experimental Wall Pressure Measurements

A. Preliminarly Choices

Some preliminarly choices have been made that allow the number of free parameters in our analysis to be reduced. We decided to perform pressure measurements on only half of the wind-tunnel

section in the cross direction, that is, the right or the left part. Indeed, most of the tests in the considered wind tunnel are carried out at zero yaw angle; if this is not the case, the tests are repeated with an opposite yaw angle to avoid spurious effects of lack of symmetry in the flow or model geometry. Thus, a lateral symmetry is always present in experimental data acquisition.

Moreover, we decided to adopt a constant number of sensors for each cross section; in the specific application to the MSWT, these are located at the center of the slats present on the wind-tunnel walls, as shown in Fig. 2. Thus, the cross distribution of the pressure sensors is uniquely determined by their number N_c and by the position of the slats over which sensors are present.

As concerns the sensor distribution in the longitudinal direction, it is clear that the pressure sensors should be clustered in the regions where high gradients are present in the flow and, thus, near the model. The inverse of the distance between a sensor and the model rotation point is determined from a Gaussian function centered at the model rotation point. Thus, the longitudinal distribution is uniquely defined by the number of sensors in that direction, N_l, and by the standard deviation σ of the Gaussian function.

To define acceptable values of the parameters, the acceptable accuracy of the correction method should be identified earlier. Let us consider that the desired accuracy of the aerodynamic force measurements is a priori fixed. The accepted global error ε_{tot} is due to different sources, as shown in Fig. 3.

When it is assumed that the optimal error distribution is that in which all error sources, at each level, are of the same order, the acceptable error due to the representation of wall pressure distribution is $|\varepsilon_{\text{pr}}| \approx \frac{1}{8}|\varepsilon_{\text{tot}}|$; ε_{pr} is defined as the difference between the values of the aerodynamic coefficients given by the FA simulation and those obtained in the tunnel simulation after correction. The assumption that the different sources of error are of the same order at each level is classically used in error analysis, for preliminarly studies. It is based on the idea that, if at a certain level the magnitude of one of the error sources is given, it is not useful to reduce significantly the importance of the other terms. In the present study, we assume as global acceptable errors the values suggested in Ref. 6, that is, ± 0.01 on the lift coefficient and ± 0.001 on the pitching moment coefficient.

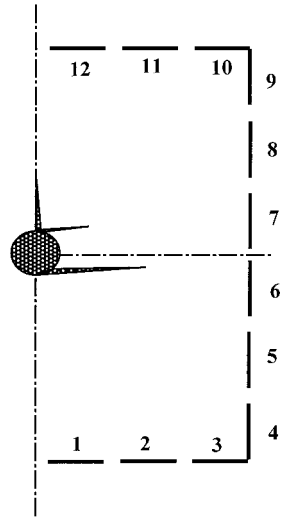

Fig. 2 Wind-tunnel cross section.

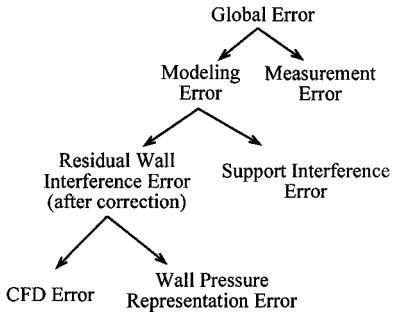

Fig. 3 Error distribution graph.

B. Sensitivity Analysis by a Potential Flow Solver

A potential flow solver[7] based on Morino's formulation has been used; its accuracy was assessed for a complete aircraft in Ref. 8.

For the tunnel simulations, boundary conditions for ideal homogeneous slotted walls have been implemented in the potential code, following the method proposed in Ref. 9. In particular, the following boundary condition is used on the wind-tunnel walls:

$$\frac{V_n}{U_\infty} = \int_{x_0}^{x} \frac{c_p}{2k}\,\mathrm{d}x \tag{1}$$

in which c_p is the pressure coefficient at the wind-tunnel wall. For the present study, we adopted the definition of k suggested in Ref. 9:

$$k = (L/\pi)\,\ell n[\sin(\pi_a/2L)]^{-1} \tag{2}$$

This boundary condition is clearly an approximation of the real behavior at the slotted walls of the MSWT. The boundary condition proposed by Berndt,[10] in which open slots are modeled by equivalent strips of ideal porous surfaces, might be more accurate.[11] However, we decided to carry out the sensitivity analysis with the earlier simpler boundary condition and to account for the effects of the particular slotted wall geometry by a suitable interpolation of sensor pressure data. A first example of different interpolation laws can be found later in this section. More accurate interpolation will be devised, for the specific application to the MSWT, by using either Navier–Stokes calculations, in which the wall geometry is exactly reproduced, or pressure measurements in the slots.

From a practical point of view, boundary condition (1) is imposed by an iterative procedure. A first simulation is carried out by setting $V_n = 0$ (solid walls), in which the c_p values at the wind tunnel walls are evaluated. Then, the values of V_n are obtained at each streamwise location x from Eq. (1) and are used as boundary conditions in a second simulation. This iterative procedure is stopped when the differences between the c_p values obtained in two successive simulations are lower than an a priori fixed value.

The analyzed geometry is the ONERA M5 configuration, shown in Fig. 4. The first analyzed condition is characterized by a Mach number $M = 0.4$ and an angle of attack $\alpha = 0$ deg (corresponding to $C_L \approx 0.25$). The aerodynamic center of the model (0.604 m from the model nose) is located on the balance rotation point. The ratio between the wing span and the wind-tunnel test section width is 0.75, and the resulting blockage factor (defined as the ratio between the cross section of the model and the wind-tunnel section) is about 1.5%.

A sensitivity analysis to the number of panels has been carried out, and all of the presented results are obtained with approximately 7000 panels (3000 on the model). The further increase of number

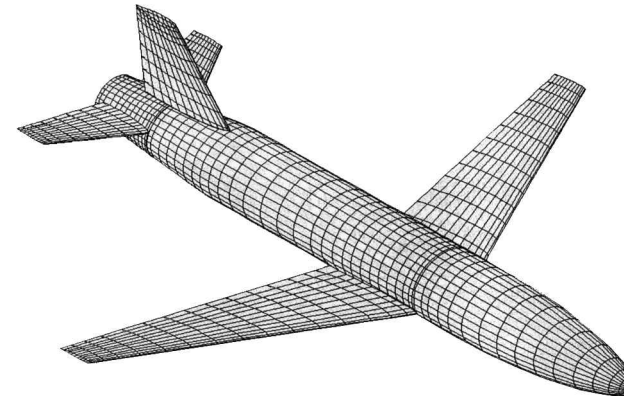

Fig. 4 ONERA M5 geometry.

of panels has been found to give differences lower than 10^{-4} for the lift coefficient C_L and 10^{-5} for the pitching moment coefficient C_m.

The lift coefficient and the pitching moment coefficient (referred to the wing aerodynamic center), obtained in the FA simulation and for the model mounted in the wind tunnel, are shown in Table 1. The resulting wall interference effects, ΔC_L and ΔC_m, are also reported.

Note that for the considered configuration the wall interference effects are rather small; hence, this test case is particularly challenging for the correction method because the required accuracy is clearly higher when we are dealing with small quantities.

As a first step in our sensitivity analysis, in the transversal direction we use all of the pressure data obtained in the wind-tunnel simulation (infinite sensors). We analyze then the sensitivity to the parameter N_l, that is, we take only N_l pressure values among those obtained in the wind-tunnel simulation, distributed as already described, with $\sigma = 2.1$. The pressure values in the remaining panels are obtained by linear interpolation of the N_l used data. The residual errors after the correction procedure are shown in Table 2, for both C_L and C_m. The residual error on both C_L and C_m decreases monotonically as the number of longitudinal sensors increases. The adopted accuracy limits (see Sec. III.A) are always verified for C_L, whereas more than 15 sensors are required for C_m.

Different values of the parameter σ have been analyzed, namely, $\sigma = 1.5$, 2.1, and 2.7, and it appeared that the residual error tends to decrease as σ decreases, that is, when the sensors are clustered near the model. However, the differences in the residual errors obtained for the same configuration with $\sigma = 1.5$ and 2.1 were found to be lower than 10^{-4} for both C_L, and C_m, and thus we can conclude that the results of the present analysis are not significantly affected by the choice of $\sigma = 2.1$.

We analyze now the sensitivity to the number and distribution of pressure sensors in the cross direction; infinite sensors are considered in the longitudinal direction. The analyzed configurations are summarized in Table 3, and the corresponding residual errors after the correction are reported in Table 4.

The residual errors on both C_L and C_m are globally higher than the corresponding errors due to a limited number of sensors in the longitudinal direction. Moreover, the behavior is not monotonic with respect to N_c; note, for instance, that the accuracy obtained with 10 sensors is lower than that given by 8 sensors in configuration 8A.

Table 1 Reference solutions for the configuration at $M = 0.4$, $\alpha = 0$ deg

Configuration	C_L	C_m
FA	0.2490	0.28666
Tunnel	0.2367	0.27538
Difference Δ	0.0123	0.01128

Table 2 Residual error for different numbers of longitudinal sensors and infinite sensors in the cross direction

N_l	ε_{pr} for C_L	ε_{pr} for C_m
25	0.00005	0.00007
20	0.00012	0.00016
15	0.00025	0.00025
10	0.00032	0.00050

Table 3 Definition of cross configurations (see Fig. 2)

N_c configuration	Slats with sensor
12	ALL
10	All except 2, 11
8A	1–3–5–6–7–8–10–12
8B	1–3–4–5–8–9–10–12
8C	1–3–4–6–7–9–10–12
6	1–3–5–8–10–12

Table 4 Residual error for different numbers of cross sensor and infinite sensors in the longitudinal direction

N_c configuration	ε_{pr} for C_L	ε_{pr} for C_m
12	−0.00028	−0.00011
10	−0.00044	−0.00021
8A	−0.00023	−0.00004
8B	−0.00110	−0.00038
8C	−0.00103	−0.00053
6	−0.00092	−0.00021

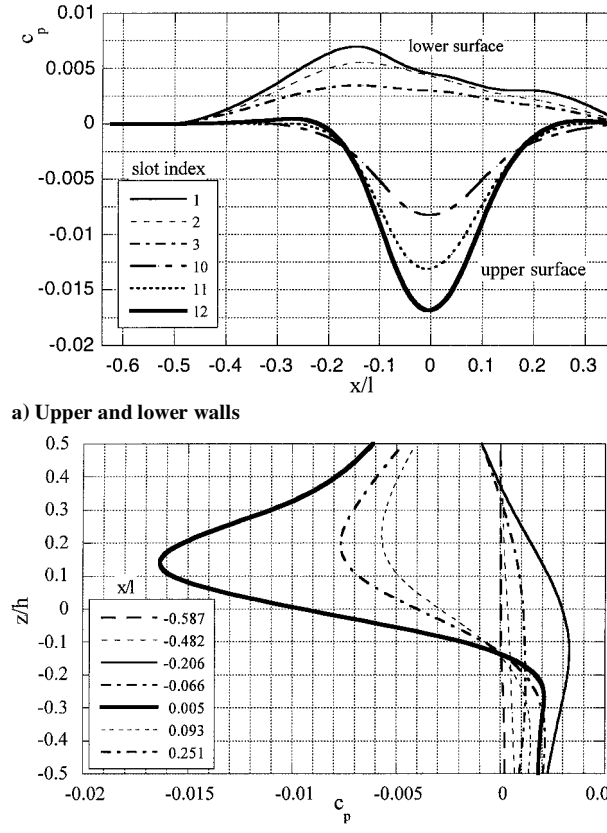

Fig. 5 Pressure coefficient along the wind-tunnel walls.

This behavior can be explained by analyzing the wall pressure distributions obtained in the wind-tunnel simulation, shown in Fig. 5. In the longitudinal direction, as expected, high gradients are present in correspondence to the model. Because in the adopted longitudinal distribution the sensors are clustered in this region, this effect is reasonably well captured also with a limited N_l. Even steeper gradients are found in the cross direction, near the model. However, in this direction, we chose to locate only one sensor per slat; thus, these gradients are ill represented because a very low number of pressure data is used in this region and they are linearly interpolated. This also explains why the correction accuracy is very sensitive to the cross location of the sensors. Thus, it appears that, to obtain an acceptable residual error with a limited N_c, a more accurate interpolation must be employed.

Thus, the following interpolation has also been used for the cross direction: a parabolic law on the upper and lower walls of the cross section (see Fig. 2), in which a symmetry condition is imposed on the centerline and cubic splines on the lateral wall.

The residual errors obtained with infinite sensors in the longitudinal direction and different N_c for this new interpolation law are reported in Table 5. By comparison with the values in Table 4, it appears that, as expected, for fixed N_c, a more accurate interpolation leads to a more accurate correction. In particular, note that now acceptable errors are obtained for all of the considered configurations.

Table 5 Residual error for different numbers of cross sensors with parabolic/cubic pressure interpolation

N_c configuration	ε_{pr} for C_L	ε_{pr} for C_m
10	0.000011	−0.000063
8A	0.000014	−0.000019
6	0.000411	0.000021

A number of different configurations have also been analyzed, by taking a limited number of sensors in both longitudinal and cross directions. The results, not reported here for the sake of brevity, show that, for both C_L and C_m, the residual error due to limited N_l and N_c, can be reasonably expressed as follows:

$$|\varepsilon_{pr}(N_l, N_c)| \approx |\varepsilon_{pr}(N_l, \infty)| + |\varepsilon_{pr}(\infty, N_c)| \quad (3)$$

This means that the two error sources are substantially uncoupled, and thus the considerations made on the basis of the earlier described analyses also hold for real configurations with limited N_l and N_c.

In the preceding analyses the experimental error in pressure measurements has not been considered because the exact pressure values obtained in the wind-tunnel simulations have been used. A sensitivity analysis to the error in pressure measurements has been carried out for a few selected configurations in terms of N_l and N_c, namely, 18×10, 18×8, 15×10, and 15×8. The cases having eight cross sensors correspond to the configuration earlier called 8A. To this aim, the wall pressure values obtained in the wind-tunnel simulation are perturbed by a priori fixed quantities. As a first investigation, the same quantity is added to all of the considered sensors, which represents the maximum error of the pressure transducers, E. The perturbed pressure values are then used in the PG simulations. This represents the situation caused by a wrong calibration of the acquisition system or of the sensors, for instance, a wrong determination of the reference pressure.

The residual error after correction increases linearly with the error in pressure measurements, as shown, for instance, in Fig. 6a, for the lift coefficient. Moreover, it is practically independent of the number and distribution of the sensors. Similar results have been obtained for the pitching moment coefficient (Fig. 6b).

In summary, the residual error after correction, due to all of the sources considered, can be expressed as

$$|\varepsilon_{pr}(N_l, N_c, E)| \approx |\varepsilon_{pr}(N_l, \infty, 0)| + |\varepsilon_{pr}(\infty, N_c, 0)| + k|E| \quad (4)$$

with k_e independent of N_l and N_c. For the analyzed configuration, k_e can be estimated to be 0.054 and −0.144, respectively, for C_L and C_m, if E is expressed in kilopascal.

However, although less realistic, a more critical situation could occur when the pressure measurement of each sensor is affected by an error $\pm E$, in which the sign is randomly distributed. For the configuration with 18×10 sensors and for $E = 0.01$ kPa, 30 different error distributions have been analyzed. We found that for 73% of the analyzed cases, the residual errors on C_L are lower than the ones obtained with a constant error equal to ± 0.01 kPa, whereas for C_m this is verified in the 98% of the studied cases. Finally, if also the value of the pressure measurement inaccuracy is varied randomly in the range $[-E, E]$, the residual errors after correction, on both C_L and C_m, are in all cases significantly lower than those obtained with constant E. Thus, expression (4) can reasonably be assumed as a conservative estimate of the residual error.

C. Choice of a Sensor Configuration

On the basis of the described sensitivity analysis, different sensor configurations satisfying the required accuracy of the correction have been identified. In particular, the configuration characterized by $N_c = 10$ and $N_l = 18$ was found to satisfy these requirements. To verify its behavior in more perturbed flow conditions, the same configuration has also been investigated at $M = 0.6$ and $\alpha = 2$ deg, corresponding to $C_L \approx 0.51$. The residual errors are reported, for both flow conditions, in Table 6.

Table 6 Residual errors for the configuration N_c =10 and N_l = 18

Flow condition	ΔC_L	ΔC_m	ε_{pr} for C_L	ε_{pr} for C_m
$M = 0.4$, $\alpha = 0$ deg	0.0123	0.01128	0.00011	0.00018
$M = 0.6$, $\alpha = 2$ deg	0.0310	0.02105	0.00016	0.00001

Table 7 Residual error for the configuration N_c = 10 and N_l = 18, without upwind sensor rows

	$M = 0.4$, $\alpha = 0$ deg		$M = 0.6$, $\alpha = 2$ deg	
Configuration	ε_{pr} for C_L	ε_{pr} for C_m	ε_{pr} for C_L	ε_{pr} for C_m
Basic	0.00011	0.00016	0.00018	0.00001
Without 1	0.00010	0.00016	0.00017	0.00001
Without 2	0.00010	0.00018	0.00019	0.00004
Without 3	0.00023	0.00061	0.00065	0.00050

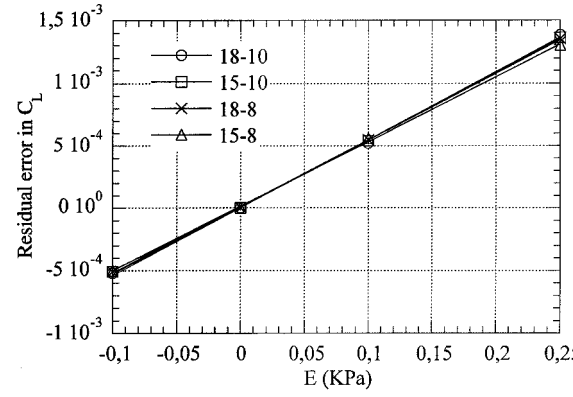

a) Lift coefficient

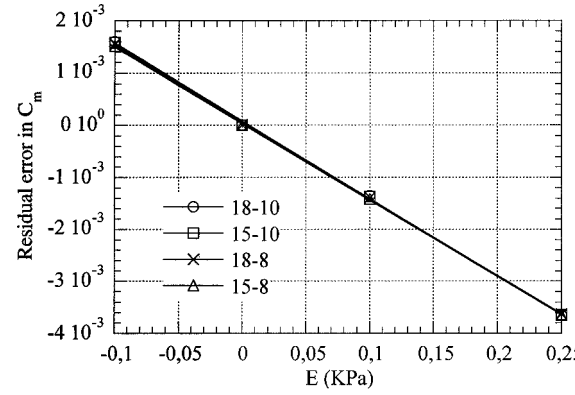

b) Pitching moment coefficient

Fig. 6 Residual error after correction as a function of the transducer error in pressure measurements.

The results show that, when the flow is more perturbed, the residual errors are of the same order or lower than in the condition used for the sensitivity analysis. This confirms that, at least for subsonic flow, conditions in which the correction to be applied is larger are less critical for the procedure.

Finally, it was noticed that the values of the pressure perturbations are negligible at the location corresponding to the most upwind transversal rows of sensors. Therefore, to further reduce the number of sensors, the earlier defined configuration in which the most upwind rows are progressively removed, is analyzed. The results are reported in Table 7 and show that the removal of the first two rows does not significantly affect the residual errors.

Therefore, a good compromise between accuracy and number of sensors is the configuration characterized by $N_c = 10$ and $N_l = 16$, in which the longitudinal sensor distribution is that obtained as described earlier with $\sigma = 2.1$ and $N_l = 18$, and the first two up-wind

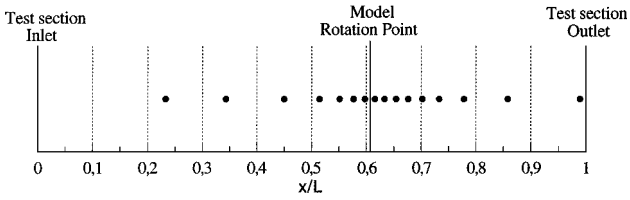

Fig. 7 Selected longitudinal distribution of sensors.

transversal rows are not used. The longitudinal distribution of sensors in this configuration is shown in Fig. 7.

IV. Conclusions

A procedure has been setup for the correction of wind-tunnel wall interference effects on the experimental measurement of aerodynamic coefficients. The correction is obtained as the difference between the values given by two numerical simulations: In the first one the flow over the model in FA conditions is simulated, and in the second one, the measured pressure values over the wind tunnel walls are used as boundary conditions.

A necessary preliminarly step is the choice of the number, location, and accuracy of the pressure measurements. A strategy has been proposed to determine these parameters, based on the same correction procedure in which the experimental part is replaced by a numerical simulation.

Some preliminarly choices have been made to reduce the number of free parameters to be determined. First, the wall pressure values are measured only on half of the wind-tunnel cross section, and only one sensor can be located on each slat. Thus, the cross distribution of the pressure sensors is uniquely determined by their number N_c and by the position of the slats over which sensors are present. The longitudinal distribution has been assumed to be Gaussian and centered at the model rotation point; hence, it is defined by the number of longitudinal sensors, N_l, and by the standard deviation σ of the Gaussian. Finally, the acceptable accuracy of the correction method has been identified, given the desired accuracy of the aerodynamic force measurements.

Then, an analysis of the sensitivity of the correction accuracy to the earlier defined parameters has been carried out using the ONERA M5 configuration in subsonic conditions and a potential flow solver. It has been found that the residual errors on the aerodynamic coefficients after the correction can be expressed as the sum of the errors due only to the limited number of sensors in the longitudinal direction and the analogous ones in the cross direction. The error in the longitudinal direction decreases monotonically as N_l increases and is only marginally sensitive to σ. Conversely, the residual error in the cross direction is not monotonic with N_c, depending on the sensor location. Moreover, the errors are globally higher than the corresponding ones in the longitudinal direction. This behavior is due to steep lateral pressure gradients present on the wind-tunnel walls and is significantly improved by using cubic/quadratic interpolations of the pressure data.

Finally, the residual errors after correction have been found to increase linearly with the error in the pressure measurements.

On the basis of this analysis, a configuration characterized by $N_l = 16$ and $N_c = 10$ has been identified, which represents a good compromise between accuracy and experimental costs.

Thus, the proposed strategy, given the desired correction accuracy, permits identification of suitable sensor configurations with reduced time and computational costs. However, the accuracy and efficiency of this strategy also must be verified in transonic conditions. This aspect will be eventually investigated by means of a Navier–Stokes solver.

References

[1] Kraft, E. M., "An Overview of Approaches and Issues for Wall Interference Assessment and Correction," CP-2319, NASA, 1983.

[2] Lynch, F. T., Crites, R. C., and Spaid, F. W., "Wall Interference, Support Interference and Flow Field Measurement," AGARD, CP-535, 1994.

[3] Lombardi, G., and Morelli, M., "Analysis of Some Interference Effects in a Transonic Wind Tunnel," *Journal of Aircraft*, Vol. 32, No. 3, 1995, pp. 501–509.

[4] Sickles W., "Wall Interference Correction for Three-Dimensional Transonic Flows," AIAA Paper 90-1408, June 1990.

[5] Lombardi, G., Salvetti M. V., and Morelli, M., "Appraisal of Numerical Methods in Predicting the Aerodynamics of Forward-Swept Wings," *Journal of Aircraft*, Vol. 35, No. 4, 1998, pp. 561–568.

[6] Steinle, F., and Stanewsky, E., "Wind Tunnel Flow Quality and Data Accuracy Requirements," AGARD, AR-184, 1982.

[7] Polito, L., and Lombardi, G., "Calculation of Steady and Unsteady Aerodynamic Loads for Wing–Body Configurations at Subcritical Speeds," *Proceedings of the AIDAA Conference*, Vol. 1, Napoli, Italy, 1983, pp. 209–222.

[8] Baston, A., Lucchesini, M., Manfriani, L., Polito, L., and Lombardi, G., "Evaluation of Pressure Distributions on an Aircraft by Two Different Panel Methods and Comparison with Experimental Measurements," *Proceedings of 15th ICAS Congress*, London, 1986, pp. 618–628.

[9] Kemp, W. B. Jr., "A Panel Method for Interference Assessment in Slotted Wall Wind Tunnel," AIAA Paper 88-2573, July 1988.

[10] Berndt, G., S. B., "Inviscid Theory of Wall Interference in Slotted Test Sections," *AIAA Journal*, Vol. 15, No. 9, 1977, pp. 1278–1287.

[11] Malmuth, N., Crites, R., Everhart, J., Newman, P., Sickles, W., "Transonic Wind Tunnel Wall Interference," AGARDograph 336, 1998.